

## Inhibitive effect of chloroquine towards corrosion of mild steel in hydrochloric acid solution

Ashish Kumar Singh · Shagufta Khan ·  
Aditya Singh · S. M. Quraishi · M. A. Quraishi ·  
Eno E. Ebenso

Received: 11 April 2012 / Accepted: 4 June 2012 / Published online: 27 June 2012  
© Springer Science+Business Media B.V. 2012

**Abstract** Corrosion inhibition of mild steel (MS) by chloroquine (CQ) in 1 M HCl was investigated using weight loss, polarization, electrochemical impedance spectroscopy (EIS) and quantum chemical techniques. The inhibitor showed 99 % inhibition efficiency at concentration of  $3.1 \times 10^{-4}$  M. Polarization studies showed that CQ is a mixed-type inhibitor. Adsorption of inhibitor molecules on the MS surface showed Langmuir adsorption isotherm. Thermodynamic parameters led to the conclusion that adsorption is predominantly chemisorption. Quantum chemical calculations were carried out to investigate the corrosion-inhibiting property of CQ. Various parameters such as energy of the highest occupied molecular orbital (HOMO) and lowest unoccupied molecular orbital (LUMO), softness of molecule, Mullikan charges on various atoms and number of electrons transferred from inhibitor molecule to metal were calculated and correlated with the inhibiting property of CQ.

---

A. K. Singh (✉) · E. E. Ebenso  
Department of Chemistry, School of Mathematical and Physical Sciences, North West University (Mafikeng Campus), Private Bag X2046, Mmabatho 2735, South Africa  
e-mail: singhac@gmail.com

S. Khan · M. A. Quraishi (✉)  
Department of Applied Chemistry, Institute of Technology, Banaras Hindu University,  
Varanasi 221005, India  
e-mail: maquraishi@rediffmail.com

A. Singh  
Department of Ceramic Engineering, Institute of Technology, Banaras Hindu University,  
Varanasi 221005, India

S. M. Quraishi  
Department of Mechanical Engineering, Institute of Technology, Banaras Hindu University,  
Varanasi 221005, India

**Keywords** PM3 semiempirical method · Electrochemical techniques · Inhibition of corrosion · Langmuir adsorption isotherm

## Introduction

Mild steel has found extensive application in various industries. Acidic solutions are used extensively in several industrial processes such as acid pickling, acid cleaning, acid scaling and oil wet cleaning [1]. Acidic solutions are highly corrosive for mild steel. It is possible to reduce the corrosion rate to safe level by adding inhibitors. There are a wide range of organic inhibitors, but unfortunately most of them are very expensive and hazardous to health. Thus, it remains an important objective to find low-cost and ecofriendly inhibitors. In this direction, exploration of drugs for their corrosion inhibition properties seems to be a viable concept. Most of the inhibitors investigated for corrosion of steels in acid solutions are heterocyclic compounds [2–5]. Recently, a few non-toxic compounds such as diethylcarbamazine, tryptamine, succinic acid, L-ascorbic acid, sulphamethaxazole, cefatrayl, disulfiram, ceftobiprole, cefuroxime, cefazolin, cefapirin, ceftazole etc. have been studied as corrosion inhibitors by our research groups [3–12] and other researchers [13–18].

The present article is devoted to the study of chloroquine (CQ) as a corrosion inhibitor for mild steel in hydrochloric acid solution using electrochemical impedance spectroscopy (EIS), potentiodynamic polarization, weight loss method and quantum chemical techniques.

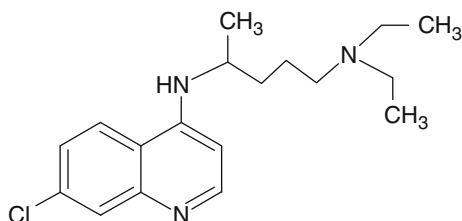
Chloroquine (CQ) is the commercial name of *N'*-(7-chloroquinolin-4-yl)-*N*,*N*-diethyl-pentane-1,4-diamine. It is used as an antimalarial. It has many adsorption centres ( $=N-$ ,  $-NH-$ ,  $-NH_2$ , aromatic ring etc.). The structure of chloroquine is shown in Fig. 1.

## Experimental

### Inhibitor

Stock solution of CQ was made in 10:1 water:ethanol mixture by volume to ensure solubility. This stock solution was used for all experimental purposes.

**Fig. 1** Chemical structure of chloroquine



## Corrosion measurements

Prior to all measurements, mild steel specimens, having composition (wt.%) C = 0.17, Mn = 0.46, Si = 0.26, S = 0.017, P = 0.019 and balance Fe, were abraded successively with emery papers from 600 to 1200 mesh/in grade. The specimens were washed thoroughly with double-distilled water, degreased with acetone and finally dried using a hot air blower. After drying, the specimens were placed in desiccators and then used for experiments. Aggressive solution of 1 M HCl was prepared by dilution of analytical-grade HCl (37 %) with double-distilled water, and all experiments were carried out in unstirred solutions. Rectangular specimens with dimensions of  $2.5 \times 2.0 \times 0.025 \text{ cm}^3$  were used in weight loss experiments, and specimens of size  $1.0 \times 1.0 \text{ cm}^2$  (exposed) with a 7.5-cm-long stem (isolated using commercially available lacquer) were used for electrochemical measurements.

## Electrochemical impedance spectroscopy

EIS tests were performed at  $308 \pm 1 \text{ K}$  in a three-electrode assembly. A saturated calomel electrode (SCE) was used as reference; a  $1\text{-cm}^2$  platinum foil was used as counterelectrode. All potentials are reported versus SCE. Electrochemical impedance spectroscopy (EIS) measurements were performed using a Gamry Instruments potentiostat/galvanostat with a Gamry framework system based on ESA 400 in the frequency range of 10–2 Hz to 105 Hz under potentiodynamic conditions, with amplitude of 10 mV peak-to-peak, using an alternating-current (AC) signal at  $E_{\text{corr}}$ . Gamry applications include software DC105 for corrosion and EIS300 for EIS measurements, and Echem Analyst version 5.50 software packages for data fitting. The experiments were carried out after 30 min of immersion in the testing solution (no deaeration, no stirring).

The inhibition efficiency of the inhibitor was calculated from the charge transfer resistance values using the following equation:

$$E_{\text{EIS}}\% = \frac{R_{\text{ct}}^i - R_{\text{ct}}^0}{R_{\text{ct}}^i} \times 100, \quad (1)$$

where  $R_{\text{ct}}^i$  and  $R_{\text{ct}}^0$  are the charge transfer resistance in presence and absence of inhibitor, respectively.

## Potentiodynamic polarization

The electrochemical behaviour of mild steel sample in inhibited and non-inhibited solution was studied by recording anodic and cathodic potentiodynamic polarization curves. Measurements were performed in 1 M HCl solution containing different concentrations of the tested inhibitor by changing the electrode potential automatically from  $-250$  to  $+250 \text{ mV}$  versus corrosion potential at scan rate of  $1 \text{ mV s}^{-1}$ . The linear Tafel segments of anodic and cathodic curves were extrapolated to the corrosion potential to obtain the corrosion current densities ( $j_{\text{corr}}$ ).

The inhibition efficiency was evaluated from the measured  $j_{\text{corr}}$  values using the following relationship:

$$E_{\text{P}}\% = \frac{j_{\text{corr}}^0 - j_{\text{corr}}^i}{j_{\text{corr}}^0} \times 100, \quad (2)$$

where  $j_{\text{corr}}^0$  and  $j_{\text{corr}}^i$  are the corrosion current density in absence and presence of inhibitor, respectively.

### Linear polarization measurement

The corrosion behaviour was studied by polarization resistance measurements ( $R_{\text{p}}$ ) in 1 M HCl solution with and without different concentrations of the studied inhibitor. The linear polarization study was carried out from cathodic potential of  $-20$  mV versus open-circuit potential (OCP) to an anodic potential of  $+20$  mV versus OCP at scan rate  $0.125$  mV  $\text{s}^{-1}$  to study the polarization resistance ( $R_{\text{p}}$ ), evaluated from the slope of the curve in the vicinity of the corrosion potential. From the evaluated polarization resistance value, the inhibition efficiency was calculated using the following relationship:

$$E_{\text{Rp}}\% = \frac{R_{\text{p}}^i - R_{\text{p}}^0}{R_{\text{p}}^i} \times 100, \quad (3)$$

where  $R_{\text{p}}^0$  and  $R_{\text{p}}^i$  are the polarization resistance in absence and presence of inhibitor, respectively.

### Weight loss measurements

Weight loss measurements were performed on rectangular mild steel samples having dimensions of  $2.5 \times 2.0 \times 0.025$  cm<sup>3</sup> by immersing the mild steel coupons into acid solution (100 mL) in absence and presence of different concentrations of CQ. After the elapsed time, the specimen were taken out, washed, dried and weighed accurately.

All tests were conducted in aerated 1 M HCl. All experiments were performed in triplicate, and average values are reported. From the evaluated corrosion rate, the surface coverage ( $\theta$ ) and inhibition efficiency ( $E_{\text{WL}}\%$ ) were calculated using

$$\theta = \frac{C_{\text{R}}^0 - C_{\text{R}}^i}{C_{\text{R}}^0}, \quad (4)$$

$$E_{\text{WL}}\% = \frac{C_{\text{R}}^0 - C_{\text{R}}^i}{C_{\text{R}}^0} \times 100, \quad (5)$$

where  $\theta$  is the surface coverage, and  $C_{\text{R}}^0$  and  $C_{\text{R}}^i$  are the corrosion rate in absence and presence of inhibitor, respectively.

### Quantum chemical calculations

Quantum chemical calculations were performed using 3D ultra 8 and MOPAC software. The quantum chemical parameters obtained were  $E_{\text{HOMO}}$ ,  $E_{\text{LUMO}}$ ,

$E_{\text{HOMO}} - E_{\text{LUMO}}$  ( $\Delta E$ ), total energy, softness ( $\sigma$ ) and the fraction of electrons transferred from the inhibitor to steel surface ( $\Delta N$ ).

## Results and discussion

### Electrochemical impedance spectroscopy (EIS)

The impedance method provides information about the kinetics of the electrode processes and simultaneously about the surface properties of the investigated systems. The shape of the impedance gives mechanistic information. The method is widely used for investigation of corrosion inhibition processes [19]. The impedance spectra are plotted for different concentrations of CQ in Fig. 2a. Nyquist plots for mild steel in 1 M HCl solution in absence and presence of different concentrations of CQ are presented in Fig. 2a. The Nyquist plots show a depressed capacitive loop in the high-frequency (HF) range and an inductive loop in the low-frequency (LF) range. A capacitive loop arises from the time constant of the electric double layer and charge transfer resistance, and an inductive loop originates from the adsorption relaxation of intermediates, which cover the reaction surface.

The HF semicircle is attributed to the time constant of charge transfer and double-layer capacitance [20, 21]. The LF inductive loop may be attributed to the relaxation process obtained by adsorption species as  $\text{Cl}_{\text{ads}}^-$  and  $\text{H}_{\text{ads}}^+$  on the electrode surface [22, 23].

To get a more accurate fit to these experimental data, the measured impedance data were analysed by fitting based on the equivalent circuit given in Fig. 2b. Excellent fit with this model was obtained for all experimental data. The equivalent circuit consists of the double-layer capacitance ( $C_{\text{dl}}$ ) in parallel with the charge transfer resistance ( $R_{\text{ct}}$ ), which is in series with the parallel inductive elements ( $L$ ) and  $R_{\text{L}}$ . The presence of  $L$  in the impedance spectra in the presence of the inhibitor indicates that mild steel is still dissolved by direct charge transfer at the CQ-adsorbed mild steel surface [24]. The value of  $L$  decreased with increasing CQ

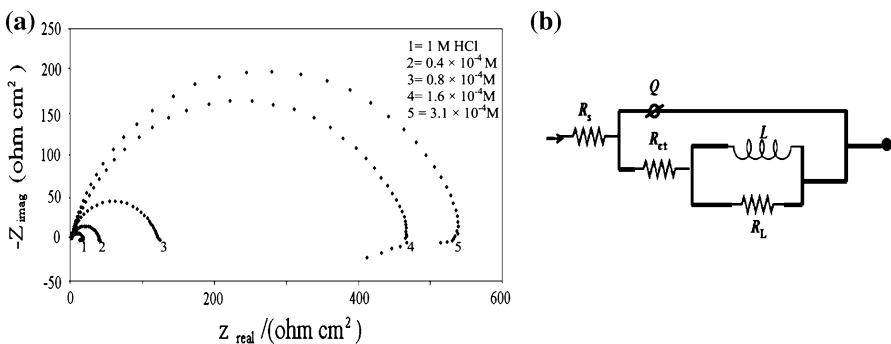


**Fig. 2** a Nyquist plots of mild steel in 1 M HCl in absence and presence of different concentrations of CQ, and b equivalent circuit for impedance measurements

concentration, as the inhibitor molecule gets strongly adsorbed onto the mild steel surface at higher concentration.

One constant-phase element (CPE) is substituted for the capacitive element to give a more accurate fit, as the obtained capacitive loop is a depressed semicircle. Depression of Nyquist semicircles is a feature of solid electrodes, often referred to as frequency dispersion and attributed to roughness and other inhomogeneities of the solid electrode [25]. The CPE is a special element whose admittance value is a function of the angular frequency ( $\omega$ ), and whose phase is independent of frequency. The admittance and impedance of the CPE are given by

$$Y_{\text{CPE}} = Y_0(i\omega)^n, \quad (6)$$

where  $Y_0$  is the magnitude of CPE,  $i$  is an imaginary number ( $i^2 = -1$ ) and  $n$  is the CPE exponent, which can be used as a gauge of the heterogeneity or roughness of the surface.

The increasing value of  $n$  with increasing inhibitor concentration reveals that the roughness of the mild steel surface decreased with increasing inhibitor concentration.

$C_{\text{dl}}$  values derived from CPE parameters according to Eq. (7) are listed in Table 1.

$$C_{\text{dl}} = Y_0(\omega_{\text{max}})^{n-1}, \quad (7)$$

where  $\omega_{\text{max}}$  is the angular frequency ( $\omega_{\text{max}} = 2\pi f_{\text{max}}$ ) at which the imaginary part of the impedance ( $-Z_i$ ) is maximal, and  $f_{\text{max}}$  is the AC frequency at maximum.

### Potentiodynamic polarization measurements

Polarization measurements were carried out to gain knowledge concerning the kinetics of the cathodic and anodic reactions. Figure 3 presents the results of the effect of CQ concentration on the cathodic and anodic polarization curves for mild steel in 1 M HCl, respectively. It can be observed that both the cathodic and anodic reactions were suppressed by addition of CQ, suggesting that CQ reduced the anodic dissolution and also retarded the hydrogen evolution reaction.

**Table 1** Different corrosion parameters obtained from electrochemical impedance spectroscopy (EIS) in absence and presence of different concentrations of CQ

Inhibitor conc. ( $\text{M} \times 10^{-4}$ )	$R_s$ ( $\Omega \text{ cm}^2$ )	$R_{\text{ct}}$ ( $\Omega \text{ cm}^2$ )	$R_L$ ( $\Omega \text{ cm}^2$ )	$\alpha$	$L$ (H)	$C_{\text{dl}}$ ( $\mu\text{F cm}^{-2}$ )	$E_{\text{EIS}}\%$
–	1.1	16.0	23.0	0.821	3.8	52.1	–
0.4	1.3	36.4	18.9	0.824	3.2	48.8	56.0
0.8	0.9	112.5	17.8	0.845	3.1	41.2	85.7
1.6	1.2	394.0	14.6	0.851	2.9	31.2	95.9
3.1	1.1	463.8	12.2	0.855	2.7	24.2	96.9

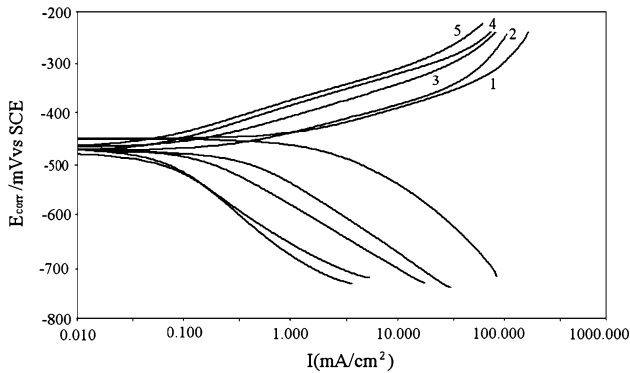


**Fig. 3** Potentiodynamic polarization curves for mild steel in 1 M HCl in absence and presence of different concentrations of CQ

Electrochemical corrosion kinetics parameters, i.e. the corrosion potential ( $E_{\text{corr}}$ ), cathodic and anodic Tafel slopes ( $b_a$ ,  $b_c$ ) and corrosion current density ( $j_{\text{corr}}$ ) obtained from extrapolation of the polarization curves, are given in Table 2.

Figure 3 presents the potentiodynamic polarization curves for mild steel in 1 M HCl in the absence and presence of various concentrations of CQ. It can be seen from Fig. 3 that, in the presence of inhibitor, the curves are shifted to lower current regions, showing the inhibition tendency of CQ. No definite trend was observed in the  $E_{\text{corr}}$  values in the presence of CQ. In the present study, the maximum shift in  $E_{\text{corr}}$  values is in the range of 27 mV, suggesting that CQ acts as a mixed-type inhibitor [26]. The values of the various electrochemical parameters derived from Tafel polarization for all the inhibitor concentrations are given in Table 2. Inspection of Table 2 reveals that the values of  $b_a$  change slightly in the presence of CQ, whereas more pronounced change occurs in the values of  $b_c$ , indicating that both the anodic and cathodic reactions are affected, but the effect on the cathodic reactions is more prominent. Thus, CQ acted as a mixed-type, but predominantly cathodic, inhibitor [27]. Increase in inhibition efficiencies with increasing concentration of CQ reveals that the inhibition action is due to adsorption on the steel surface, and the adsorption is known to depend on the chemical structure of the inhibitor.

#### Linear polarization measurements

Polarization resistance ( $R_p$ ) values were determined from the slope of potential–current lines. The  $R_p$  values were used to calculate the inhibition efficiencies ( $E_{R_p}$ %) using the relationship

$$E_{R_p}\% = \frac{R_p^i - R_p^0}{R_p^i} \times 100,$$

where  $R_p^0$  and  $R_p^i$  are the polarization resistance in absence and presence of inhibitor,

**Table 2** Different corrosion parameters obtained for mild steel in 1 M HCl in absence and presence of different concentrations of CQ

Inhibitor conc. ( $M \times 10^{-4}$ )	Weight loss data			Polarization data		Tafel data				
	Weight loss ( $\text{mg cm}^{-2}$ )	$E_{\text{WL}}\%$	$C_{\text{R}}$	$R_{\text{p}}$ ( $\Omega \text{ cm}^2$ )	$E_{\text{Rp}}\%$	$-E_{\text{corr}}$ (mV vs. SCE)	$j_{\text{corr}}$ ( $\mu\text{A cm}^{-2}$ )	$b_{\text{a}}$ (mV $\text{dec}^{-1}$ )	$b_{\text{c}}$ (mV $\text{dec}^{-1}$ )	$E_{\text{p}}\%$
–	21.0	–	155.8	7.6	–	448	1500	69	132	–
0.4	6.1	70.9	45.3	46.0	83.4	472	302	67	148	79.0
0.8	1.2	94.2	8.9	129.2	94.0	467	106	71	157	93.0
1.6	0.8	96.0	5.9	316.0	97.6	475	36	62	178	95.2
3.1	0.2	99.0	1.5	482.0	98.4	465	31	65	181	97.9

respectively. The inhibition efficiencies and polarization resistance parameters are presented in Table 2.

### Weight loss measurements

#### *Effect of inhibitor concentration*

The variation of the corrosion rate ( $C_{\text{R}}$ ) and inhibition efficiency ( $E_{\text{WL}}\%$ ) with inhibitor concentration is shown in Fig. 4a. It is observed that CQ showed its maximum efficiency ( $\sim 99\%$ ) at  $3.1 \times 10^{-4}$  M. Better inhibition efficiency at higher concentration may be attributed to greater coverage of metal by inhibitor molecules.

#### *Effect of acid concentration*

The effect of acid concentration on the corrosion behavior of mild steel in the presence of  $3.1 \times 10^{-4}$  M inhibitor concentration was studied, and the results are shown in Fig. 4b. It is clear that change in the acid concentration from 0.5 to 2.0 M results in the inhibition efficiency varying from 99.1 to 97.8%. This change in inhibition suggests that the compound is an effective corrosion inhibitor in acid solution at the studied concentration of acid solution.

#### *Effect of temperature*

The values of inhibition efficiency obtained from weight loss measurements for  $3.1 \times 10^{-4}$  M inhibitor concentrations in 1.0 M HCl are shown in Fig. 4c. From Fig. 4c, it can be seen that the inhibition efficiency decreased with increasing temperature, indicating desorption of inhibitor molecules [28].



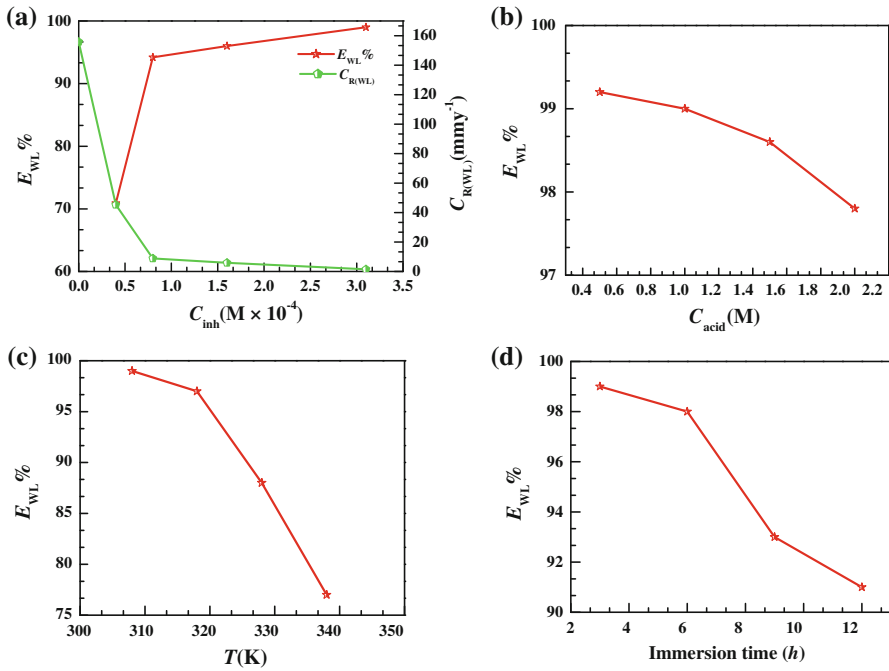


**Fig. 4** Variation of inhibition efficiency of CQ obtained from weight loss measurements with **a** concentrations of CQ, **b** acid concentration, **c** solution temperature and **d** immersion time

*Effect of immersion time*

The variation of inhibition efficiency with immersion time in HCl is shown in Fig. 4d. It is found that the inhibition efficiency decreases with time. It is obvious that the weight loss varied linearly with immersion period in plain acid and inhibited acid, showing the absence of insoluble product on the steel surface.

*Thermodynamic and activation parameters*

The dependence of the corrosion rate on temperature can be expressed by Arrhenius equation and transition-state equation as

$$\log(C_R) = \frac{-E_a}{2.303RT} + \log \lambda, \tag{8}$$

$$C_R = \frac{RT}{Nh} \exp\left(\frac{\Delta S^*}{R}\right) \exp\left(\frac{-\Delta H^*}{RT}\right), \tag{9}$$

where  $E_a$  is the apparent activation energy,  $\lambda$  is the Arrhenius pre-exponential factor,  $R$  is the gas constant,  $h$  is Planck’s constant and  $N$  is the Avogadro number.

Figure 5 depicts Arrhenius plots for mild steel immersed in 1 M HCl in absence and presence of  $3.1 \times 10^{-4}$  M concentration of CQ. Table 3 includes activation parameters. The data show that the activation parameters of corrosion of mild steel

in uninhibited solution are higher than in inhibited solution, indicating that CQ exhibited low inhibition efficiency at elevated temperature. The shift towards positive values of entropy ( $\Delta S^*$ ) implies that the activated complex in the rate-determining step represents dissociation rather than association, meaning that disordering increases on going from reactants to the activated complex.

The free energy of adsorption ( $\Delta G_{\text{ads}}^0$ ) calculated using the following equations is also given in Table 3:

$$\Delta G_{\text{ads}}^0 = -RT \ln(55.5K_{\text{ads}}), \quad (10)$$

$$K_{\text{ads}} = \frac{\theta}{C_{\text{inh}}(1 - \theta)}, \quad (11)$$

where  $\theta$  is the degree of coverage of the metal surface,  $C_{\text{inh}}$  is the inhibitor concentration in  $\text{mol}^{-1}$ ,  $R$  is a constant,  $T$  is temperature and 55.5 is the concentration of water in solution in  $\text{mol}^{-1}$  [29].

The  $\Delta G_{\text{ads}}^0$  value of the inhibitor is found to be  $-42 \text{ kJ mol}^{-1}$ . Generally, values of  $\Delta G_{\text{ads}}^0$  around  $-20 \text{ kJ mol}^{-1}$  or lower are consistent with electrostatic interaction between the charged molecules and the charged metal (physisorption); those around  $-40 \text{ kJ mol}^{-1}$  or higher involve charge sharing or transfer from organic molecules to the metal surface to form a co-ordinated type of bond (chemisorption) [30, 31]. The calculated value of  $\Delta G_{\text{ads}}^0$  is near  $-40 \text{ kJ mol}^{-1}$ , indicating, therefore, that CQ adsorbed onto mild steel in 1 M HCl solution by both predominantly by chemical process. The negative values of  $\Delta G_{\text{ads}}^0$  indicate spontaneous adsorption of inhibitor onto the surface of mild steel [32].

The enthalpy of adsorption can be calculated from the Gibbs–Helmholtz equation [33]:

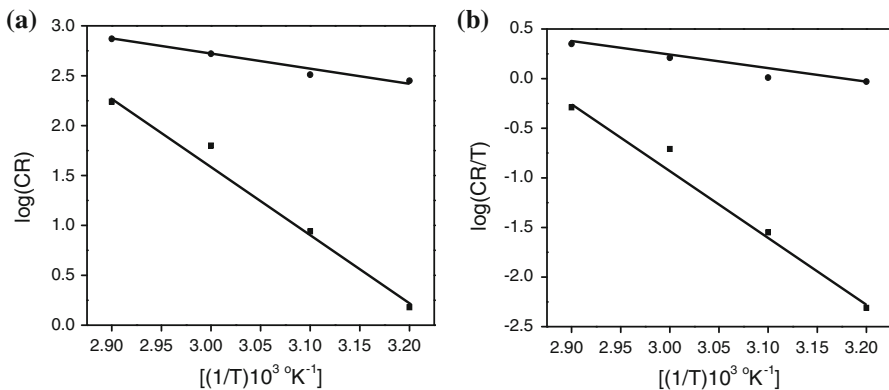


**Fig. 5** Arrhenius plots for **a**  $\log C_R$  versus  $1/T$  and **b**  $\log C_R/T$  versus  $1/T$  in absence and presence of  $3.1 \times 10^{-4} \text{ M}$  concentration of CQ

**Table 3** Values of activation and thermodynamic adsorption parameters

Inhibitor conc. (M × 10 <sup>-4</sup> )	$E_a$ (kJ mol <sup>-1</sup> )	$\Delta H^*$ (kJ mol <sup>-1</sup> )	$\Delta S^*$ (J K <sup>-1</sup> mol <sup>-1</sup> )	$\Delta G_{\text{ads}}^0$ (kJ mol <sup>-1</sup> )	$\Delta H_{\text{ads}}^0$ (kJ mol <sup>-1</sup> )
1 M HCl	28.13	25.64	-116.75	-	-
3.1 × 10 <sup>-4</sup> M	134.7	132.02	182.02	-42.70	-17.4

$$\left[ \frac{\partial \left( \frac{\Delta G_{\text{ads}}^0}{T} \right)}{\partial T} \right]_P = - \frac{\Delta H_{\text{ads}}^0}{T^2}. \quad (12)$$

This equation can be arranged as follows:

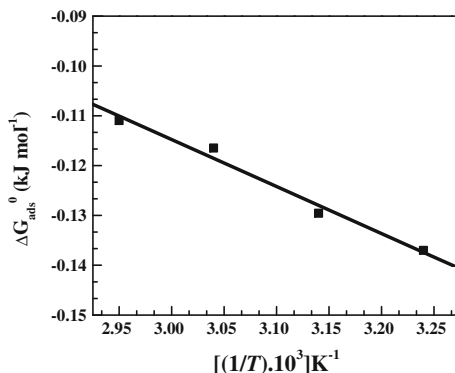
$$\frac{\Delta G_{\text{ads}}^0}{T} = \frac{\Delta H_{\text{ads}}^0}{T} + K_{\text{ads}}. \quad (13)$$

The variation of  $\Delta G_{\text{ads}}^0/T$  with  $1/T$  gives a straight line with a slope that equals  $\Delta H_{\text{ads}}^0$  (Fig. 6). It can be seen from the figure that  $\Delta G_{\text{ads}}^0/T$  decreases with  $1/T$  in a linear fashion. The calculated values are depicted in Table 3. The negative sign of  $\Delta H_{\text{ads}}^0$  in HCl solution indicates that adsorption of inhibitor molecule is an exothermic process. Generally, an exothermic adsorption process signifies either physi- or chemisorption, while an endothermic process is attributable unequivocally to chemisorption [34]. In the presented case, the calculated value of  $\Delta H_{\text{ads}}^0$  for adsorption of CQ is  $-17.4 \text{ kJ mol}^{-1}$ , indicating that this inhibitor can be considered to adsorb by a mixture of both processes. It is well known that organic inhibitors establish inhibition by adsorption onto the metal surface. Adsorption of an inhibitor is influenced by the chemical structure of the organic compound, the nature and surface charge of the metal, the distribution of charge in the molecule and the type of aggressive media considered [35, 36]. Physical adsorption requires the presence of an electrically charged metal surface and charged species in the bulk of solution. In the case of chemisorption, the process involves charge sharing or charge transfer from the inhibitor molecule to the metal surface. This is possible in case of positive as well as negative charges on this surface. The presence, with a transition metal, having vacant and low-energy electron orbital, of an inhibitor molecule having relatively loosely bound electrons or heteroatom with lone-pair electrons facilitates this adsorption [37].

### Quantum chemical calculations

Quantum chemical calculations have proved to be a very powerful tool for studying corrosion inhibition mechanisms [38, 39]. Quantum chemical parameters obtained from calculations affect the inhibition efficiency of inhibitors, including the energies of the highest occupied molecular orbital ( $E_{\text{HOMO}}$ ) and lowest unoccupied molecular orbital ( $E_{\text{LUMO}}$ ), the separation energy ( $E_{\text{LUMO}} - E_{\text{HOMO}}$ ), dipole, total

**Fig. 6** Plot of  $\Delta G_{\text{ads}}^0/T$  versus  $1/T$



energy (TE), softness ( $\sigma$ ) and the fraction of electrons transferred from the inhibitor to steel surface ( $\Delta N$ ). They are listed in Tables 4 and 5.  $\Delta N$  and  $\sigma$  may be calculated by the following equations [40]:

$$\Delta N = \frac{\chi_{\text{Fe}} - \chi_{\text{inh}}}{2(\eta_{\text{Fe}} - \eta_{\text{inh}})}, \quad (14)$$

$$\sigma = \frac{1}{\eta},$$

where  $\chi$  and  $\eta$  are the absolute electronegativity and absolute hardness, respectively, and may be calculated by the following equations:

$$\eta = \frac{1}{2(I - A)}, \quad (15)$$

$$\chi = \frac{1}{2(I + A)}, \quad (16)$$

where  $I$  and  $A$  are the ionization potential and electron affinity, respectively. According to Koopmans' theorem [41, 42], the first ionization energy of a molecular system is equal to the negative of the orbital energy of the HOMO. Koopmans' theorem also allows the calculation of electron affinities as the LUMO of the respective system [43]. Thus, the orbitals of the inhibitor molecule are related to the ionization potential and electron affinity as follows:

$$I = -E_{\text{HOMO}},$$

$$A = -E_{\text{LUMO}}.$$

The three-dimensional structure of CQ is shown in Fig. 7a. The frontier molecular density distribution of CQ is presented in Fig. 7b, c. It is confirmed that, the more negative the atomic charges of the adsorbed centre, the more easily the atom donates its electrons to the unoccupied orbital of metal [44]. Table 4 shows that the Mulliken charge on  $N_{11}$  is greater than that on  $N_7$  or  $N_{17}$ . Thus, CQ can be adsorbed on the metal surface by donating its lone pair of electrons (present on more

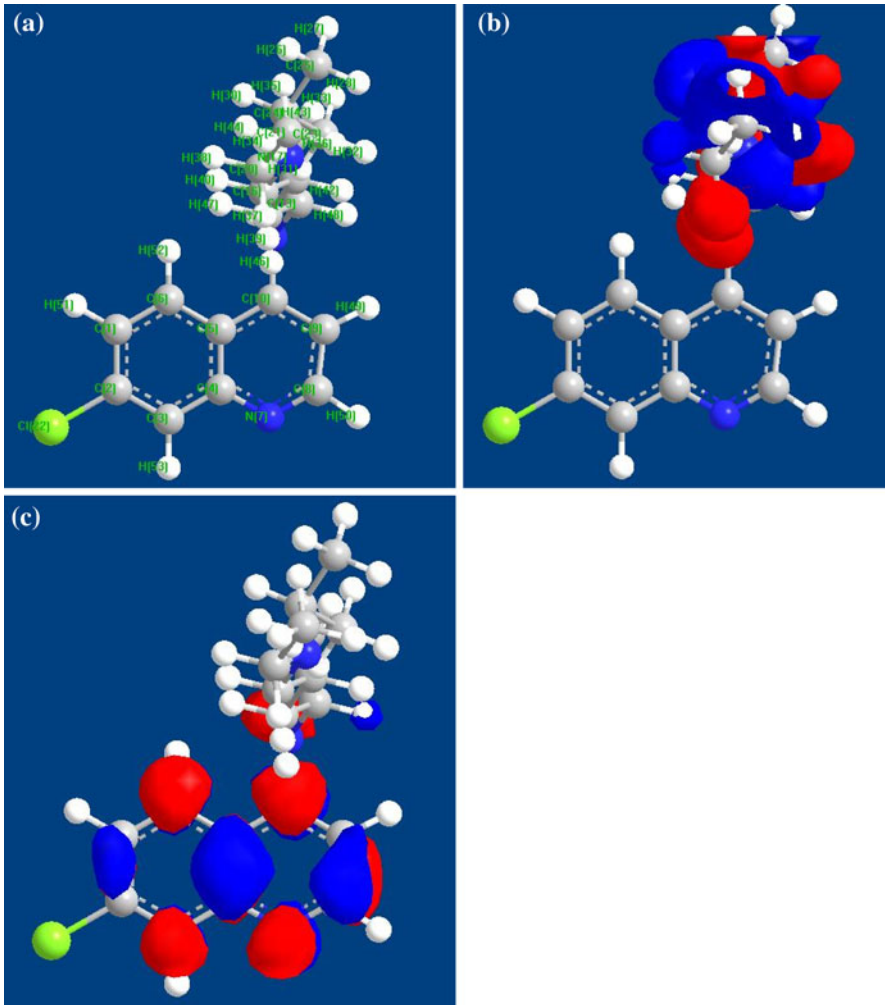


**Fig. 7** **a** Three-dimensional structure of CQ. **b** Frontier molecular orbital density distribution of CQ-HOMO. **c** Frontier molecular orbital density distribution of CQ-LUMO

negative nitrogen atoms) to vacant d orbital of metal atom. A hard molecule has a large energy gap, and a soft molecule has a small energy gap. Soft molecules are more reactive than hard molecules, in general. The calculated softness value of CQ (11.76) shows that it is an appreciably soft molecule. Moreover, the gap between the

**Table 4** Quantum chemical parameters for CQ

HOMO (eV)	LUMO (eV)	$\Delta E$ (eV)	$\mu$ (D)	TE (kcal)	$\sigma$ (softness)	$\Delta N$
-6.69	-0.75	5.94	3.74	-2408.52	11.76	1.6

**Table 5** Mulliken charges on various atoms of CQ

C1	C2	C3	C5	C6	N7	C8	C9	N11	C14	C15	N17	C20	C21	C22	C23	C24	C25
-0.19	-0.05	-0.15	-0.13	-0.15	-0.22	-0.05	-0.28	-0.55	-0.29	-0.30	-0.16	-0.29	-0.55	-0.04	-0.45	-0.37	-0.27

LUMO and HOMO energy levels of the molecules is another important factor that should be considered. Excellent corrosion inhibitors are usually those organic compounds that not only donate electrons to unoccupied orbital of the metal surface but also accept free electrons from the metal [45, 46]. It is well established in the literature that, the higher the HOMO energy of the inhibitor, the greater its tendency to offer electrons to unoccupied d orbital of the metal, and the higher its corrosion inhibition efficiency. Additionally, the lower the LUMO, the easier it is accept electrons from the metal surface. CQ has high  $E_{\text{HOMO}}$  and low  $E_{\text{LUMO}}$ , suggesting that CQ could be both electron acceptor and electron donor. The electric/orbit density distribution of the HOMO and LUMO for CQ is shown in Fig. 7. It is clear from the figure that the electron density of the HOMO is localized mainly on nitrogen atoms outside of the ring, whereas the electron density of the LUMO is mainly localized on the quinoline ring. The fraction of electron transfer from CQ to metal is 1.6.

### Mechanism of inhibition

The adsorption of organic compounds can be described by two main types of interactions: physical adsorption and chemisorption. The presence of a transition metal, having vacant, low-energy electron orbital, and an inhibitor with molecules having relatively loosely bound electrons or heteroatom with a lone pair of electrons is necessary for the inhibiting action [47]. In hydrochloric acid, CQ could be protonated. Thus, protonated and neutral molecules of CQ could be adsorbed on the metal surface through different mechanisms. Generally, two modes of adsorption could be assumed. The steel surface is positively charged in HCl [48]. So, it is difficult for protonated CQ to approach the positively charged steel surface, but  $\text{Cl}^-$ , having a smaller degree of hydration, easily get adsorbed onto the metal surface. Protonated CQ can be adsorbed on the negatively charged steel surface through electrostatic forces. According to the results of thermodynamic and quantum chemical calculations, chemisorption is another mode of adsorption. This mechanism involves displacement of water molecules from the metal surface and sharing of electrons between the metal and iron.

### Conclusions

1. The inhibition efficiency of CQ increases with increasing inhibitor concentration. The inhibitor showed maximum inhibition efficiency of 99.0 % at  $3.1 \times 10^{-4}$  M concentration of the inhibitor.
2. Impedance studies and adsorption isotherm showed that its inhibition properties are due to adsorption at the metal surface.
3. Potentiodynamic polarization proved its mixed-type inhibitor property. CQ is an efficient inhibitor for corrosion of mild steel in hydrochloric acid.
4. The quantum parameters show that the HOMO and LUMO energies are correlated to the inhibition efficiency. High value of  $E_{\text{HOMO}}$  is likely to indicate

a tendency for the inhibitor to donate electrons to empty molecular orbital of low energy. Meanwhile, the energy of the lowest unoccupied molecular orbital,  $E_{LUMO}$ , indicates the ability of the inhibitor molecule to accept electrons. So, the lower the value of  $E_{LUMO}$ , the greater the probability that the molecule will accept electrons. The inhibition efficiency increases with increasing HOMO and decreasing LUMO energy values.

- From the calculated values of  $\Delta N$  and softness it is evident that CQ effectively decreases the corrosion rate by electron donation.

## References

- M. Lagrenee, B. Mernari, M. Bouanis, M. Traisnel, F. Bentiss, Study of the mechanism and inhibiting efficiency of 3,5-bis(4-methylthiophenyl)-4H-1,2,4-triazole on mild steel corrosion in acidic media. *Corros. Sci.* **44**, 573 (2002)
- M. Abdallah, H.E. Megahed, A.M. Atia, Pyridine derivatives as corrosion inhibitors for dissolution of iron electrode in tartaric acid. *J. Electrochem. Soc. India* **35**, 47 (1998)
- M.A. Quraishi, M.Z.A. Rafiquee, S. Khan, N. Saxena, *J. Appl. Electrochem.* **37**, 1153 (2007)
- F. Bentiss, M. Lebrini, H. Vezin, M. Lagrenee, *Mater. Chem. Phys.* **87**, 18 (2004)
- A. Popova, E. Sokolova, S. Raicheva, M. Christov, AC and DC study of the temperature effect on mild steel corrosion in acid media in the presence of benzimidazole derivatives. *Corros. Sci.* **45**, 33 (2003)
- A.K. Singh, M.A. Quraishi, Investigation of the effect of disulfiram on corrosion of mild steel in hydrochloric acid solution. *Corros. Sci.* **53**, 1288 (2011)
- A.K. Singh, M.A. Quraishi, Adsorption properties and inhibition of mild steel corrosion in hydrochloric acid solution by ceftobiprole. *J. Appl. Electrochem.* **41**, 7–18 (2011)
- A.K. Singh, M.A. Quraishi, E.E. Ebenso, Inhibitive effect of cefuroxime on the corrosion of mild steel in hydrochloric acid solution. *Int. J. Electrochem. Sci.* **6**, 5676 (2011)
- A.K. Singh, M.A. Quraishi, Effect of cefazolin on the corrosion of mild steel in HCl solution. *Corros. Sci.* **52**, 152 (2010)
- A.K. Singh, E.E. Ebenso, M.A. Quraishi, Adsorption behaviour of cefapirin on mild steel in hydrochloric acid solution. *Int. J. Electrochem. Sci.* **7**, 2320 (2012)
- A.K. Singh, M.A. Quraishi, Inhibitive effect of diethylcarbazine on the corrosion of mild steel in hydrochloric acid, *Corros. Sci.* **52**, 1529 (2010)
- A.K. Singh, E.E. Ebenso, Effect of ceftazolin on the corrosion of mild steel in HCl solution. *Int. J. Electrochem. Sci.* **7**, 2349 (2012)
- G. Moretti, F. Guidi, G. Grion, Tryptamine as a green iron corrosion inhibitor in 0.5 M deaerated sulphuric acid. *Corros. Sci.* **46**, 387 (2004)
- F.C. Giacomelli, C. Giacomelli, M.F. Amadori, V. Schmidt, A. Spinelli, Inhibitor effect of succinic acid on the corrosion resistance of mild steel: electrochemical, gravimetric and optical microscopic studies. *Mater. Chem. Phys.* **83**, 124 (2004)
- E.S. Ferreira, C. Giacomelli, F.C. Giacomelli, A. Spinelli, Evaluation of the inhibitor effect of l-ascorbic acid on the corrosion of mild steel. *Mater. Chem. Phys.* **83**, 129 (2004)
- E.E.F. El Sherbini, Sulphamethoxazole as an effective inhibitor for the corrosion of mild steel in 1.0 M HCl solution. *Mater. Chem. Phys.* **61**, 223 (1999)
- M.S. Morad, Inhibition of iron corrosion in acid solutions by cefatrexyl: behaviour near and at the corrosion potential. *Corros. Sci.* **50**, 436 (2008)
- M. Abdallah, Antibacterial drugs as corrosion inhibitors for corrosion of aluminium in hydrochloric solution. *Corros. Sci.* **4**(6), 2004 (1981)
- S. Martinez, M.M. Huksovic, A nonlinear kinetic model introduced for the corrosion inhibitive properties of some organic inhibitors. *J. Appl. Electrochem.* **33**, 1137 (2003)
- A.K. Singh, M.A. Quraishi, Study of some bidentate schiff bases of isatin as corrosion inhibitors for mild steel in hydrochloric acid solution. *Int. J. Electrochem. Sci.* **7**, 3222 (2012)



21. C. Deslouis, B. Tribollet, G. Mengoli, M.M. Musiani, Electrochemical behaviour of copper in neutral aerated chloride solution. I. Steady-state investigation. *J. Appl. Electrochem.* **18**, 374 (1988)
22. A.K. Singh, M.A. Quraishi, Inhibiting effects of 5-substituted isatin-based Mannich bases on the corrosion of mild steel in hydrochloric acid solution. *J. Appl. Electrochem.* **40**, 1293 (2010)
23. A.K. Singh, M.A. Quraishi, The effect of some bis-thiadiazole derivatives on the corrosion of mild steel in hydrochloric acid. *Corros. Sci.* **52**, 1373 (2010)
24. V.P. Singh, P. Singh, A.K. Singh, Synthesis, structural and corrosion inhibition studies on cobalt(II), nickel(II), copper(II) and zinc(II) complexes with 2-acetylthiophene benzoylhydrazone. *Inorg. Chim. Acta* **379**, 56 (2011)
25. A.K. Singh, Inhibition of mild steel corrosion in hydrochloric acid solution by 3-(4-((Z)-indolin-3-ylideneamino)phenylimino)indolin-2-one. *Ind. Eng. Chem. Res.* **51**, 3215 (2012)
26. A.K. Singh, M.A. Quraishi, Investigation of adsorption of isoniazid derivatives at mild steel/hydrochloric acid interface: electrochemical and weight loss methods. *Mater. Chem. Phys.* **123**, 666 (2010)
27. A.K. Singh, S.K. Shukla, M. Singh, M.A. Quraishi, Inhibitive effect of ceftazidime on corrosion of mild steel in hydrochloric acid solution. *Mater. Chem. Phys.* **129**, 68 (2011)
28. M.A. Quraishi, A. Singh, V. Singh, D.K. Yadav, A.K. Singh, Green approach to corrosion inhibition of mild steel in hydrochloric acid and sulphuric acid solutions by the extract of *Murraya koenigii* leaves. *Mater. Chem. Phys.* **122**, 114 (2010)
29. J. Flis, T. Zakroczyński, Impedance study of reinforcing steel in simulated pore solution with tannin. *J. Electrochem. Soc.* **143**, 2458 (1996)
30. M. Stern, A.L. Geary, Electrochemical polarization. *J. Electrochem. Soc.* **104**, 56 (1957)
31. G.K. Gomma, M.H. Wahdan, Schiff bases as corrosion inhibitors for aluminium in hydrochloric acid solution. *Mater. Chem. Phys.* **39**, 209 (1995)
32. M. Abdallah, Rhodamine azosulpha drugs as corrosion inhibitors for corrosion of 304 stainless steel in hydrochloric acid solution. *Corros. Sci.* **44**, 717 (2002)
33. A.K. Singh, S.K. Shukla, M.A. Quraishi, E.E. Ebenso, Investigation of adsorption characteristics of *N,N'*-(methylimino)dimethylidene]di-2,4-xylylidine as corrosion inhibitor at mild steel/sulphuric acid interface. *J. Taiwan Inst. Chem. Eng.* (2011). doi:[10.1016/j.jtice.2011.10.012](https://doi.org/10.1016/j.jtice.2011.10.012)
34. B. Donnelly, T.C. Downie, R. Grzeskowiak, H.R. Hamburg, D. Short, The effect of electronic delocalization in organic groups R in substituted thiocarbamoyl RCSNH<sub>2</sub> and related compounds on inhibition efficiency. *Corros. Sci.* **18**, 109 (1978)
35. F. Bentiss, C. Jama, B. Mernari, H.E. Attari, L.E. Kadi, M. Lebrini, M. Traisnel, M. Lagrèe, Corrosion control of mild steel using 3,5-bis(4-methoxyphenyl)-4-amino-1,2,4-triazole in normal hydrochloric acid medium. *Corros. Sci.* **51**, 1628 (2009)
36. S. Muralidharan, M.A. Quraishi, S.K.V. Iyer, The effect of molecular structure on hydrogen permeation and the corrosion inhibition of mild steel in acidic solutions. *Corros. Sci.* **37**, 1739 (1995)
37. A.K. Singh, M.A. Quraishi, Effect of 2,2' benzothiazoyl disulfide on the corrosion of mild steel in acid media. *Corros. Sci.* **51**, 2752 (2009)
38. D. Wang, S. Li, Y. Ying, M. Wang, H. Xiao, Z. Chen, Theoretical and experimental studies of structure and inhibition efficiency of imidazoline derivatives. *Corros. Sci.* **41**, 1911 (1999)
39. G. Bereket, C. Ogretir, C. Ozsahin, Quantum chemical studies on the inhibition efficiencies of some piperazine derivatives for the corrosion of steel in acidic medium. *J. Mol. Struct. (THEOCHEM)* **663**, 39 (2003)
40. R.M. Issa, M.K. Awed, F.M. Atlam, Quantum chemical studies on the inhibition of corrosion of copper surface by substituted uracils. *Appl. Surf. Sci.* **255**, 2433 (2008)
41. V.S. Sastri, J.R. Perumareddi, Molecular orbital theoretical studies of some organic corrosion inhibitors. *Corrosion* **53**, 671 (1996)
42. T. Koopmans, Über die Zuordnung von Wellenfunktionen und Eigenwerten zu den Einzelnen Elektronen Eines Atoms. *Physica* **1**, 104 (1934)
43. A. Szabo, N.S. Ostlund, *Modern Quantum Chemistry; Introduction to Advanced Electronic Structure*, Dover, 49 (1996)
44. C.T. Wang, S.H. Chen, H.Y. Ma, C.-S. Qi, Protection of copper corrosion by carbazole and *N*-vinylcarbazole self-assembled films in NaCl solution. *J. Appl. Electrochem.* **33**, 179 (2003)
45. J. Fang, J. Li, Quantum chemistry study on the relationship between molecular structure and corrosion inhibition efficiency of amides. *J. Mol. Struct. (Theochem)* **593**, 179 (2002)
46. P. Zhao, Q. Liang, Y. Li, Electrochemical, SEM/EDS and quantum chemical study of phthalocyanines as corrosion inhibitors for mild steel in 1 mol/l HCl. *J. Appl. Surf. Sci.* **252**, 1596 (2005)

47. A.H. Mehaute, G. Grepv, Introduction to transfer and motion in fractal media: the geometry of kinetics. *Solid State Ionic* **9**, 17 (1989)
48. L. Tang, X. Li, L. Li, G. Mu, G. Liu, Interfacial behavior of 4-(2-pyridylazo) resorcin between steel and hydrochloric acid. *Surf. Coat. Technol.* **201**, 384 (2006)